Cytotoxic activity and cellular processing in human ovarian carcinoma cell lines of a new platinum(II) compound containing a fluorescent substituted propylene diamine ligand

Patricia Marqués-Gallego, Hans Den Dulk, Jaap Brouwer, Stefania Tanase, Ilpo Mutikainen, Urho Turpeinen, Jan Reedijk

Accepted Manuscript

Title: Cytotoxic activity and cellular processing in human ovarian carcinoma cell lines of a new platinum(II) compound containing a fluorescent substituted propylene diamine ligand

Authors: Patricia Marqués-Gallego, Hans den Dulk, Jaap Brouwer, Stefania Tanase, Ilpo Mutikainen, Urho Turpeinen, Jan Reedijk

PII: S0006-2952(09)00331-1
DOI: doi:10.1016/j.bcp.2009.04.027
Reference: BCP 10162

To appear in: *BCP*

Received date: 16-3-2009
Revised date: 17-4-2009
Accepted date: 24-4-2009

Please cite this article as: Marqués-Gallego P, Dulk H, Brouwer J, Tanase S, Mutikainen I, Turpeinen U, Reedijk J, Cytotoxic activity and cellular processing in human ovarian carcinoma cell lines of a new platinum(II) compound containing a fluorescent substituted propylene diamine ligand, *Biochemical Pharmacology* (2008), doi:10.1016/j.bcp.2009.04.027

Revised **Biochemical Pharmacology, April 2009**

Cytotoxic activity and cellular processing in human ovarian carcinoma cell lines of a new platinum(II) compound containing a fluorescent substituted propylene diamine ligand.

Patricia Marqués-Gallego,[a] *Hans den Dulk,*[a] *Jaap Brouwer,*[a] *Stefania Tanase,*[a] *Ilpo Mutikainen,*[b] *Urho Turpeinen,*[b] *Jan Reedijk* [a*]

[a] Leiden Institute of Chemistry, Gorlaeus Laboratories, Leiden University, PO Box 9502, 2300 RA Leiden, The Netherlands

[b] Department of Chemistry, Laboratory of Inorganic Chemistry, University of Helsinki, P. O. Box 55, A. I. Virtasenaukio 1, 00014 Helsinki, Finland

Corresponding author: reedijk@chem.leidenuniv.nl

Fax: (+31) 71-5274671

Abstract

A new fluorescent platinum(II) compound containing the N,N'-bis-(anthracen-9-ylmethyl)propane-1,3-diamine as a carrier ligand has been designed, synthesized and characterized. High cytotoxic activity of *cis*-[Pt(bapda)Cl_2] is observed in A2780 and A2780R cells (human ovarian carcinoma sensitive and cisplatin-resistant, respectively). Nevertheless, cross-resistance to platinum from *cis*-[Pt(bapda)Cl_2] in the A2780R cells was found. To study the role of GSH towards inactivation of *cis*-[Pt(bapda)Cl_2], GSH-depleted and non-depleted A2780R cells were used in several *in vitro* studies. The results suggest that *cis*-[Pt(bapda)Cl_2] is not susceptible to the inactivation by GSH. Cellular processing of bapda and *cis*-[Pt(bapda)Cl_2] was followed using fluorescence microscopy in the A2780, the A2780R and GSH-depleted A2780R cells. Interestingly, differences in the cellular processing followed by fluorescence microscopy between normal and GSH-depleted A2780R cells have been observed for the carrier ligand. Sequestration of these compounds in acidic lysosomes is visible after incubation in most cases, and no fluorescence was observed in the nucleus. Interaction of *cis*-[Pt(bapda)Cl_2] with calf thymus DNA strongly suggests that the this new platinum(II) compound intercalates between the DNA base pairs. Additionally, the reaction of *cis*-[Pt(bapda)Cl_2] with 9-ethylguanine appears to be very slow, as studied by ^{1}H and ^{195}Pt-NMR spectroscopy.

Keywords Cytotoxic activity; Fluorescence microscopy; Nucleobases; Platinum resistance, Glutathione

Abbreviations bapda: N,N'-bis(anthracen-9-ylmethyl)propane-1,3-diamine; MTT: 3-(4,5-dimethyltriazol-2-yl)-2,5-diphenyl-2H-tetrazolium bromide; 9-EtG: 9-ethylguanine; GSH: glutathione; L-BSO: L-buthionine-*S*,*R*-sulfoximine; pEC_{50} values = -log EC_{50}; RF: resistance factor (EC_{50} A2780R/EC_{50} A2780); PBS: phosphate buffered saline

1. Introduction

In the last three decades many efforts have been dedicated to establish the factors related to the antitumor activity of different platinum compounds. Even though the molecular mechanistic studies of cisplatin and analogues have been largely developed [1, 2], the cellular response to these compounds is still poorly understood. Much of the current understanding of the mechanism of action of platinum-based drugs comes from studies with cisplatin. One interesting approach proposed recently, based on a fluorescein-labeled cisplatin derivative [3], has brought new insights on the cellular response against cisplatin antitumor agent with the use of fluorescence microscopy [4, 5]. Thus, studies concerning antitumor drugs and cellular response open new options towards the design and development of new platinum compounds [6-9].

The strategy of the present study deals with the coordination of a platinum(II) moiety to the fluorescent carrier ligand N,N'-bis(anthracen-9-ylmethyl)propane-1,3-diamine (abbreviated as bapda). It has been shown that the coordination of platinum(II) to fluorescent ligands is a successful approach to synthesize fluorescent platinum drugs [6, 10]. Moreover, coordination compounds containing propane-1,3-diamine have been used as model anticancer-agents to study the interaction with DNA [11]. The N-methyl substituted trimethylenediamines, N,N'-dimethylpropane-1,3-diamine, and derivates have been used in the synthesis of platinum(II) complexes giving a six-membered chelating ring with the platinum(II) ion [12, 13]. Thus, chelation of the bapda carrier ligand to the platinum(II) ion through the aliphatic diamines moiety would be expected.

The present contribution describes synthesis and detailed structural characterization of a new fluorescent platinum(II) compound, the *cis*-[Pt(bapda)Cl_2]. In addition, cytotoxic studies of this compound have been performed and compared to cisplatin, as well as to the free bapda, in several human cancer cell lines. The possible interaction of the *cis*-[Pt(bapda)Cl_2] compound with nucleobases has been explored with the use of the 9-ethylguanine as a DNA model base. Moreover, the interaction of *cis*-[Pt(bapda)Cl_2] with calf thymus DNA, as determined by fluorescence titration, has been explored. The cellular processing of *cis*-[Pt(bapda)Cl_2] and the ligand bapda using

fluorescent microscopy is also reported. The implication of the GSH in the cellular processing of *cis*-[Pt(bapda)Cl_2] in human ovarian carcinoma cisplatin-resistant (A2780R) cells has been explored, as a potential resistance mechanism.

2. Experimental Section

2.1. Physical Measurements

C, H and N analyses were performed with a Perkin-Elmer 2400 series II analyzer. Infrared spectra (4000-300 cm^{-1}) were recorded on a Perkin-Elmer Paragon 1000 FTIR spectrometer equipped with a Golden Gate ATR device, using the reflectance technique (resolution 4 cm^{-1}). All NMR spectra were recorded with a 300-MHz Bruker DPX 300 spectrometer with a 5-mm multi-nucleus probe. The temperature was kept constant at 298 K for standard spectra, while the temperature was changed to 310 K to mimic *in vitro* studies, by a variable-temperature unit. ^{195}Pt chemical shifts was referenced to $Na_2[PtCl_6]$ (! = 0 ppm).

2.2. Materials and Reagents

The compound K_2PtCl_4 was obtained from Johnson & Matthey (Reading, U.K). All other chemicals and solvents were reagent-grade commercial materials and were used as received.

2.3. Synthesis of ligand and platinum compound

2.3.1. Synthesis of bapda

The ligand N,N'-bis(anthracen-9-ylmethyl)propane-1,3-diamine (abbreviated as bapda) was prepared by reported methods [14]. ^{1}H NMR (DMF-d_7): ! (ppm) = 8.54 (2H, s), 8.45 (4H, m), 8.08 (4H, m), 7.49 (8H, m), 4.69 (4H, s), 3.44 (2H,s)2.98 (4H, t), 1.84 (2H, m); anal. for [$C_{33}H_{30}N_2$] ½ H_2O: % found (calculated) C 85.9(85.5), H 6.4 (6.7), N 6.1 (6.0).

2.3.2.Synthesis of *cis*-[Pt(bapda)Cl_2]

To a stirred solution of bapda (109 mg, 0.24 mmol) in 2.5 ml DMF, a filtered aqueous solution of K_2PtCl_4 (100 mg, 0.24 mmol) was added. The reaction mixture was stirred two days in dark at room temperature to afford an orange solution. The resulting pale-yellow precipitate was

washed with water, ethanol, and diethyl ether and dried in vacuum. Crystalline product from diffusion of n-hexane into a THF solution of the compound was obtained. Yield 46% (79 mg). ^{1}H NMR (DMF-d_7): ! (ppm) = 9.08 (4H, d), 8.82 (2H, s), 8.22 (4H, d), 7.79 (4H, t), 7.64 (4H, t), 6.18 (2H, s), 5.71 (2H, d), 2.15 (2H, d), 1.43 (2H, d) 1.12 (2H, t); ^{195}Pt NMR (DMF-d_7):! (ppm) = -2186; anal. for [$C_{33}H_{30}N_2PtCl_2$]!1.5 THF : % found (calculated) C 55.5 (56.5), H 4.9 (5.1), N 3.7 (3.4).

2.4. X-ray Crystallographic Analysis and Data collection

Crystal data, data collection parameters, and structure refinement details are given in Table S-1, Supporting Information. A crystal was selected for the X-ray measurement and mounted to the glass fiber using the oil drop method, and data were collected at 173 K on a Nonius Kappa CCD diffractometer (Mo K! radiation, graphite monochromator, ! = 0.71073 Å). The intensity data were corrected for Lorentz and polarization effects and for absorption. The programs COLLECT [15], SHELXS-97, and SHELXL-97 [16] were used for data reduction, structure solution and structure refinement respectively. The 3D coordinates have been submitted to the CSD as a CIF file (CCDC 711124); these data can be obtained free of charge from The Cambridge Crystallographic Data Centre via www.ccdc.cam.ac.uk/data_request/cif.

2.5. Cell culture conditions and drug cytotoxicity assays

The human ovarian carcinoma cell line A2780 and its cisplatin resistant counterpart A2780R were grown as monolayers at 37 °C in a 7% CO_2 atmosphere, and were maintained in continuous logarithmic culture in Dulbecco´s modified Eagle´s Medium (DMEM) (Gibco BRL ^{TM}, Invitrogen Corporation, The Netherlands) supplemented with 10% heat inactivated fetal calf serum (Hyclone, Perbio Science, The Netherlands), penicillinG Sodium (100 units/ml: Dufecha, Biochemie BV, The Netherlands), streptomycin (100 µg/ml: Dufecha, Biochemie BV, The Netherlands) and Glutammax 100x (Gibco BRL ^{TM}, The Netherlands).

The cytotoxicity assays in A2780 and A2780R cells have been performed as previously described [17]. For GSH-depleted A2780R cytotoxicity assays the cells were seeded in 96-wells flat

bottom microtiter plates using medium containing 50 μM L-BSO, as previously described [18]. The cytotoxicity assays in A2780, A2780R and GSH-depleted A2780R cells were performed in parallel and all the cytotoxic assays were repeated five times to confirm reproducibility.

The results were analysed and the pEC_{50} values (EC_{50} is the drug concentration that produces 50% of the maximum possible response) were determined with the GraphPad Prism™ analysis software package (Graph- Pad Software, San Diego, USA) using non-linear regression (sigmoidal dose response, variable slope). The resistance factor (RF) was calculated by dividing EC_{50} in the resistant variant by the EC_{50} in the respective sensitive cell line.

In addition, the cytotoxicity of *cis*-[Pt(bapda)Cl_2], and its free ligand, were studied (PCN (Tavapharmachemie) Nederland) by means of a colorimetric microculture assay (SRB assay) [19] in seven well-characterized human tumor cell lines containing examples of breast (MCF7 and EVSA-T), colon (WIDR), ovarian (IGROV), melanoma (M19 MEL), renal (A498), and non-small cell lung cancer (H226) as previously described [20]. The IC_{50} values in the ! M range are summarized in Table S-2 (see Supporting Information). The cell lines WIDR, M19, A498, IGROV and H226 belong to the currently used anticancer screening panel of the National Cancer Institute, USA. The MCF7 cell line is estrogen (ER)+/progesterone (pgR)+ and the cell line EVSA-T is (ER)-/(pgR).

2.6. Interaction of *cis*-[Pt(bapda)Cl_2] with GSH

To establish the possible reactivity of *cis*-[Pt(bapda)Cl_2] towards glutathione, *cis*-[Pt(bapda)Cl_2] and GSH were allowed to react in a 1:4 molar ratio in DMF/PBS at 310 K, and the reaction was monitored by ^{195}Pt NMR spectroscopy for 24 h.

2.7. Reaction of *cis*-[Pt(bapda)Cl_2] with 9-Ethylguanine

The *cis*-[Pt(bapda)Cl_2] (2.44 mg, 3.4 mmol) was allowed to react with 9-ethylguanine (9-EtG, 1.2 mg, 6.7 mmol) in DMF-d_7 at 310 K to investigate how this compound interact with nucleobases. *Cis*-[Pt(bapda)Cl_2] and 9-EtG were both dissolved in DMF-d_7 and ^{1}H NMR spectra

were recorded at 310 K and followed over time. After 24 h of reaction the ^{195}Pt NMR spectrum at 310 K was recorded.

2.8. DNA fluorescence titration

Fluorescence titration of *cis*-[Pt(bapda)Cl_2] was performed as described previously [10]. Small aliquots of a concentrated calf thymus DNA solution were added to 50 ! M solutions of *cis*-[Pt(bapda)Cl_2] ranged from 0:1 to 4:1 base pairs:*cis*-[Pt(bapda)Cl_2]. Fresh solutions of *cis*-[Pt(bapda)Cl_2] in DMF diluted with phosphate buffer were prepare fresh and the titration spectra were recorded after mixing.

2.9. Digital Fluorescence Microscopy

2.9.1. Cellular processing studies

Fluorescence microscopy experiments in living cells were performed in the pair of human ovarian carcinoma A2780 and A2780R cell lines. For the living cell observations the cells were grown in 35 mm culture dish to 30-50% confluence in red phenol-free Dulbecco´s modified Eagle´s Medium (DMEM) (Gibco BRL ^{TM}, Invitrogen Corporation, The Netherlands) supplemented with 10% heat inactivated fetal calf serum (Hyclone, Perbio Science, The Netherlands), penicillinG Sodium (100 units/ml: Dufecha, Biochemie BV, The Netherlands), streptomycin (100 µg/ml: Dufecha, Biochemie BV, The Netherlands) and Glutammax 100x (Gibco BRL ^{TM}, The Netherlands). Before the incubation with the compounds, the cells were washed twice with PBS. Subsequently, the compounds were added to the cells at a final concentration of 10 µM in serum-free medium for 15 min at 37 °C and 7% CO_2 atmosphere. After incubation the cells were washed twice with PBS, and drug-free red phenol-free complete medium is added to the cells. Phase contrast and the corresponding fluorescence images were taken at different time points after incubation at 37 °C and 5.2% CO_2 atmosphere. After imaging the medium was refreshed, and the cells were kept at 37 °C in a 7% CO_2 incubator to study the accumulation 24 h after incubation with bapda or *cis*-[Pt(bapda)Cl_2] compounds.

Pictures were taken using a microscope (IX81; Olympus The Netherlands) with ×60 objective (Olympus, The Netherlands). The temperature of the culture medium was controlled between 36 and 37 °C by an objective heater and a heated ring surrounding the culture chamber. The CO_2 atmosphere was kept at 5.2% during imaging. To detect fluorescence signal of bapda ligand and *cis*-[Pt(bapda)Cl_2] a filter for λ_{ex} 377 nm; time exposure = 10 ms was used. Digital images were taken with cooled CCD camera (F-View, Olympus The Netherlands). Images were processed by Cell M software.

2.9.2. Staining of lysosomes

Lyso Tracker Red DND-99 (Molecular Probes, Leiden, The Netherlands) was used to stain the vesicles observed in the cytosol of both A2780 and A2780R cells. The staining was performed 24 h after incubation with the corresponding compound. Lyso Tracker Red DND-99 was added to the culture medium in a final concentration of 50 nM. After 15 min of incubation with the dye, the cells were washed twice with PBS, and complete phenol red-free medium was added before imaging. For detecting fluorescence of Lyso Tracker localized in lysosomes TRITC-filter (!$_{ex}$ 573 nm; time exposure = 10 ms) was used.

2.10. Statistical analysis

For statistical comparison in the cytotoxic activity against A2780 and A2780R cell lines, the Student's *t*-test was performed. A *p*-value < 0.05 was considered statistically significant.

3. Results

3.1. General characterization

The *cis*-[Pt(bapda)Cl_2] was characterized by several physical methods, such as IR, ^{1}H and ^{195}Pt NMR spectroscopy. In addition, single crystals suitable for X-Ray diffraction were obtained and the crystal structure of the platinum(II) compound has been determined and is described below.

The IR spectrum of *cis*-[Pt(bapda)Cl_2] shows the two bands expected for !$_{as}$(Pt-Cl) and !$_{s}$(Pt-Cl) in a *cis* conformation at 322 and 328 cm^{-1}. In addition, the N-H and C-H stretching region

contains three peaks (3200-3000 cm^{-1}) [13]. The ^{1}H NMR spectra of the carrier ligand and the *cis*-[Pt(bapda)Cl_2] in DMF-d_7 were recorded and compared. Significant changes upon coordination of the ligand bapda to the platinum(II) ion are observed. The H_2 and H_4 protons appear at 2.98 ppm (triplet) in the ligand spectrum, while the spectrum of *cis*-[Pt(bapda)Cl_2] shows two doublets at 2.15 and 1.43 ppm, respectively. In addition the H_3 peak is shifted from 1.84 to 1.09 in the platinum(II) compound. Moreover, the singlet at 4.69 ppm corresponding to H_6 and $H_{6'}$ protons in the ligand displays a clear shift to 5.71 ppm, which indicates clearly the coordination to the platinum(II) ion. Next to this peak, a broad singlet at 6.18 ppm corresponding to the NH protons can be observed. It is worth to note that both anthryl moieties appear as identical in the ^{1}H NMR spectrum, in agreement with the symmetry of the platinum(II) compound. In addition, different diastereoisomers from the chiral nitrogen formed upon coordination of bapda to platinum(II) ion were not observed in a DMF-d_7 solution of *cis*-[Pt(bapda)Cl_2] at 298 K. The coordination of the platinum(II) ion to bapda is also visible from the ^{195}Pt NMR spectrum, which displays a single peak at -2186 ppm corresponding to a [N_2Cl_2] environment [21].

The stability of *cis*-[Pt(bapda)Cl_2] compound in solution has been followed in time in DMF-d_7 by ^{1}H NMR and ^{195}Pt NMR spectroscopy. Changes over time were not observed (spectra not shown); therefore, the biological studies reported below were performed using a concentrated stock solution of *cis*-[Pt(bapda)Cl_2] compound in DMF and diluting it in cell medium at the desired concentration when needed.

3.2. X-ray Analysis and Structure description

Single crystals of *cis*-[Pt(bapda)Cl_2] were obtained by slow diffusion of n-hexane into a THF solution containing *cis*-[Pt(bapda)Cl_2]. Selected bond lengths and angles for *cis*-[Pt(bapda)Cl_2] are listed in Table 1.

The X-ray crystallographic analysis of a single crystal shows two crystallographically independent, but almost identical molecules in the asymmetric unit and 1.5 tetrahydrofurane

molecules (one ordered THF and one disordered THF, refined with occupancy factor 0.5), with a final composition of $\{[Pt(bapda)Cl_2)\}_2](THF)_{1.5}$, which crystallizes in a monoclinic $P2_1/n$ space group (Fig. 1). The solid-state crystal structure of *cis*-[Pt(bapda)Cl_2] shows the nitrogen atoms of the coordinated (now) chiral diamines to have the R and S configuration, respectively. The plane of the platinum(II) coordination is defined by the two aliphatic nitrogens atoms and the two chloride ligands. Both mononuclear units differ only slightly in the angles formed between the plane of each anthryl ring and the metal plane. The angle N1-Pt1-N5 of 95.29(18)° was found to be the largest distortion for a square-planar configuration. The platinum(II)-amine chelate forms a six-membered chelate ring, which adopts a chair conformation (Fig. 1). The dihedral angles of the Pt1-N1-N5 and C2-C3-C4 planes with respect to the N1-C2-N5-C4 plane are 32.5(2) and 62.3(2)°, respectively. These angles and the Pt-Cl and Pt-N bond lengths (Table 1) in *cis*-[Pt(bapda)Cl_2]can be compared to the ones found by Odoko *et al*. [22]; for the *cis*-[Pt(tn)Cl_2] (tn stands for propane-1,3-diamine).

Table 1. Selected bond lengths [Å] and angles [º] for the different units *cis*-[Pt(bapda)Cl_2] and relevant hydrogen bonding parameters of *cis*-[Pt(bapda)Cl_2].

Bond lengths		*Bond angles*	
Pt1 – Cl1	2.3321(15)	N1 – Pt1 – N5	95.29(18)
Pt1 – Cl2	2.3211(15)	N1 – Pt1 – Cl1	87.55(14)
Pt1 – N1	2.088(4)	N5 – Pt 1 – Cl2	85.37(12)
Pt1 – N5	2.094(4)	Cl1 – Pt1 – Cl2	91.75(5)
N1 – C2	1.503(7)		
N5 – C4	1.494(6)		
Pt2 – Cl3	2.3347(14)	N21 – Pt2 – N25	95.29(18)
Pt2 – Cl4	2.3206(15)	N21 – Pt2 – Cl3	84.88(13)
Pt2 – N21	2.065(4)	N25 – Pt2 – Cl4	85.70(13)
Pt2 – N25	2.075(5)	Cl4 – Pt2 – Cl3	94.13(5)
N25 – C24	1.507(7)		
N21 – C22	1.505(7)		

D-H•••A	D•••A [Å]	D-H•••A [deg]
N5--H5A..Cl3	3.434(5)	132
N6--H6A..Cl2	3.445(5)	139

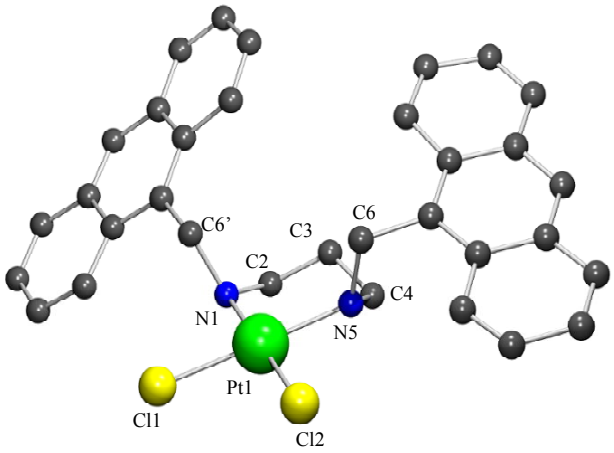

Fig. 1. PLATON/POVRAY view of one of the two *cis*-[Pt(bapda)Cl_2] entities. Hydrogen atoms and THF solvent molecules have been omitted for clarity.

A view of the molecular packing along the *c* direction reveals the presence of intermolecular contacts in the form of π-π stacking interactions (3.792 !) established between two anthracene rings that belong to two platinum(II) mononuclear units of the same type (Figure S1, Supporting Information). The two anthracene rings are parallel, and the angle between the ring of the anthracene and the centroid vector is 24.28°. In addition, the interaction between two platinum centers with a distance of 3.867(1) !, and moderately strong intermolecular N-H!!!Cl hydrogen bonds are observed in the crystal packing (Figure S1, Supporting Information).

3.3. Cytotoxicity in human ovarian carcinoma cell lines

The cytotoxic activity of *cis*-[Pt(bapda)Cl_2], the platinum-free ligand bapda, and cisplatin as reference compound against A2780 and A2780R cell lines were studied. The EC_{50} (mM) values after 48 h incubation are listed in Table 2.

The *cis*-[Pt(bapda)Cl_2] displays a high cytotoxic activity against both the human ovarian carcinoma sensitive and cisplatin-resistant cell lines. Moreover, significant difference ($p < 0.05$) between the cytotoxic activity in A2780 cell line of *cis*-[Pt(bapda)Cl_2] and the ligand bapda was found, indicating that the coordination compound is significantly more active against the cisplatin-

sensitive human ovarian carcinoma A2780 cells. In addition, *cis*-[Pt(bapda)Cl_2] displays the same level of cytotoxic activity as cisplatin in A2780 cells, where significant differences ($p > 0.05$) were not observed. Both bapda and *cis*-[Pt(bapda)Cl_2] improve the cytotoxic activity against A2780R as compared to cisplatin treatment (Table 2), however, significant differences ($p < 0.001$) between A2780 and A2780R cytotoxic activity of *cis*-[Pt(bapda)Cl_2] were observed, suggesting cross-resistance to platinum of *cis*-[Pt(bapda)Cl_2] in the A2780R cells, which is indicated also by the resistance factor (RF > 2) listed in Table 2.

Table 2. pEC_{50} and EC_{50} values after 48 h incubation and with *cis*-[Pt(bapda)Cl_2], bapda, and cisplatin as a reference compound in human ovarian carcinoma cell lines A2780 and A2780R (pEC_{50}, mean ± SD, n = 4 - 5).

Test compound	***A2780***	***A2780R***	***RF****	***A2780R-L-BSO***
bapda				
pEC_{50}	2.46±0.0	2.40±0.0		2.17±0.09
EC_{50} (mM)	3	5	1.1	$6.8\ 10^{-3}$
	$3.5\ 10^{-3}$	$4.0\ 10^{-3}$		
Pt(bapda)Cl_2				
pEC_{50}	2.64±0.1	2.15±0.0		2.19±0.07
EC_{50} (mM)	3	6	3.1	$6.5\ 10^{-3}$
	$2.3\ 10^{-3}$	$7.1\ 10^{-3}$		
cisplatin				
pEC_{50}	2.64±0.1	1.70±0.0		2.12±0.06
EC_{50} (mM)	3	5	8.7	$7.6\ 10^{-3}$
	$2.3\ 10^{-3}$	$20.0\ 10^{-3}$		

*RF = EC_{50} (A2780R)/ EC_{50} (A2780)

A2780R-L-BSO = A2780R cells pre- and co-incubated with L-BSO during cytotoxic studies

Elevated levels of GSH provide some cancer cells resistance against platinum cancer drugs such as cisplatin [7], and the binding to such molecules, prior the binding to DNA, has been

presented earlier from our laboratory [23-25]. As mentioned above, cis-[Pt(bapda)Cl_2] shows cross-resistance to platinum after 48 h incubation in A2780R cells. It is well known that the resistance mechanisms against platinum drugs are multifactorial, and four mechanisms for drug resistance have been proposed [26]: (i) inhibition of drug uptake or increased drug efflux, (ii) inactivation of the drug by thiol-containing molecules (metallothionein and/or glutathione) within the cells, (iii) accelerated repair of chemotherapy-induced cellular damage, and (iv) inhibition of cell death pathways. To investigate the implication of the GSH in our results, depletion of GSH levels by L-buthionine-*S,R*-sulfoximine (L-BSO) in A2780R was investigated towards cytotoxic activity of *cis*-[Pt(bapda)Cl_2] (Table 2). Not significant differences were found ($p > 0.05$) when the cytotoxic activity of *cis*-[Pt(bapda)Cl_2] in normal A2780R and GSH-depleted A2780R cells are compared.

Surprisingly, the depletion of GSH levels in A2780R cells influences the ligand bapda cytotoxic activity, with significant differences between normal A2780R cells and L-BSO treated A2780R cells. Moreover, it is important to note that the cytotoxic activity of cisplatin against GSH-depleted A2780R is significantly different from that of non-L-BSO treated cells ($p < 0.05$). This suggests that, under the studied conditions, the GSH levels in A2780R cells contribute to the cisplatin resistance during the cisplatin incubation. The modulation factor (MF = EC_{50} (A2780R)/ EC_{50} (A2780R-L-BSO)) of 2.6 is in agreement with literature data [18].

In addition to the cytotoxic activity against human ovarian carcinoma cell lines, it has been also investigated whether *cis*-[Pt(bapda)Cl_2] is complementary to cisplatin against a wider range of cancer cell lines. Therefore, the cytotoxic activity of *cis*-[Pt(bapda)Cl_2], the ligand bapda, and cisplatin were tested in a larger panel of human cancer cell lines (PCN Tavapharmachemie, The Netherlands). The IC_{50} values are listed in Table S-2 (see Supporting Information). *Cis*-[Pt(bapda)Cl_2] indeed shows a higher activity than cisplatin in all the cell lines tested, with the only exception of the IGROV cell line. Additionally, ligand bapda shows lower cytotoxicity compared to that of *cis*-[Pt(bapda)Cl_2] in most of the cell lines, with the exception of the H226 (non-small lung

cancer) cell line. The biological activity of *cis*-[Pt(bapda)Cl_2] and ligand bapda may stem from the interaction with the nuclear DNA; however, the differences in the cytotoxicity are small.

3.4. Interaction of *cis*-[Pt(bapda)Cl_2] with GSH

The platinum(II) compound was reacted with an excess of GSH as described above, and the reaction was followed with ^{195}Pt-NMR spectroscopy. No interaction between *cis*-[Pt(bapda)Cl_2] and GSH was detected, finding only a constant single peak at -2182 ppm corresponding to unreacted *cis*-[Pt(bapda)Cl_2] up to 24 h (serial spectra not shown).

3.5. Reaction with 9-Ethylguanine

The reaction of 9-EtG with *cis*-[Pt(bapda)Cl_2] results in the slow formation of small amounts of [Pt(bapda)(9-EtG)Cl]Cl after 10 h of reaction; nevertheless, the original *cis*-[Pt(bapda)Cl_2] remains the major species in solution (Fig. 2), even after 12 days of reaction, and only 20% of a Pt-9EtG species is obtained over this time. The ^{195}Pt NMR spectrum after 24 h of reaction was recorded, giving two peaks: one at -2181 ppm corresponding to the unreacted *cis*-[Pt(bapda)Cl_2], and a new small peak at -2335 ppm; which corresponds to the platinum-9-EtG adduct product of the reaction (as expected for a [N_3Cl] environment; See Fig. S2, supporting Information) [21]. In addition to the NMR spectroscopy, ESI-MS of the DMF-d_7 solution after 24 h of reaction shows the formation of $[Pt(bapda)(9\text{-}EtG)Cl]^+$ species, as confirmed by a m/z with platinum isotopic pattern at 864. Moreover, a peak at m/z = 686 corresponding to $[Pt(bapda)Cl]^+$ is observed as well (Fig. S3, Supporting Information).

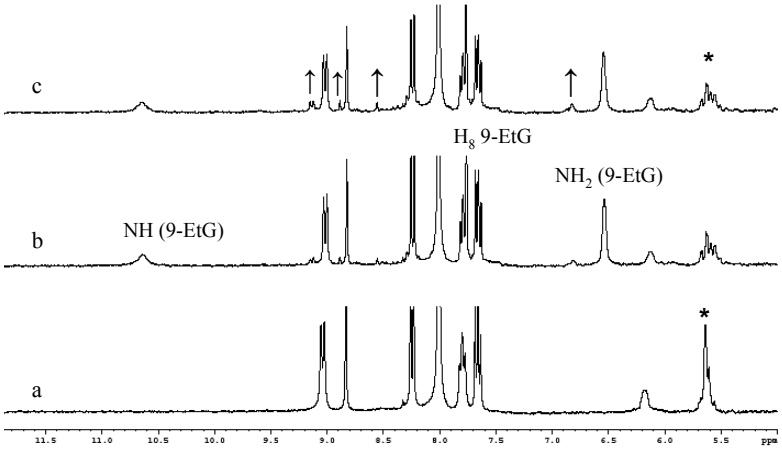

Fig. 2. Aromatic region of the ^{1}H NMR spectrum (300 MHz) of (a) *cis*-[Pt(bapda)Cl_2] in DMF-d_7 at 310 K (b) reacted with 2 eq. 9-EtG 24 h after mixed, and (c) 48 h after mixed. (↑) reaction product. (*)H_6 and $H_{6'}$ modification upon 9-EtG addition.

3.6. DNA fluorescence titration

Fluorescence quenching of platinum compounds containing intercalating agents in the presence of DNA has been described in the literature [6]. DNA titration experiments displays a clear quenching on the fluorescence emission of *cis*-[Pt(bapda)Cl_2] (!$_{ex}$ = 370 nm) with the addition of small amounts of a concentrated calf thymus DNA solution (Fig. 3) This observation suggests that *cis*-[Pt(bapda)Cl_2] interacts with DNA primarily via intercalation.

The interaction between ligand bapda and DNA was also studied, giving also a clear quenching of the fluorescence emission upon addition of calf thymus DNA (data not shown).

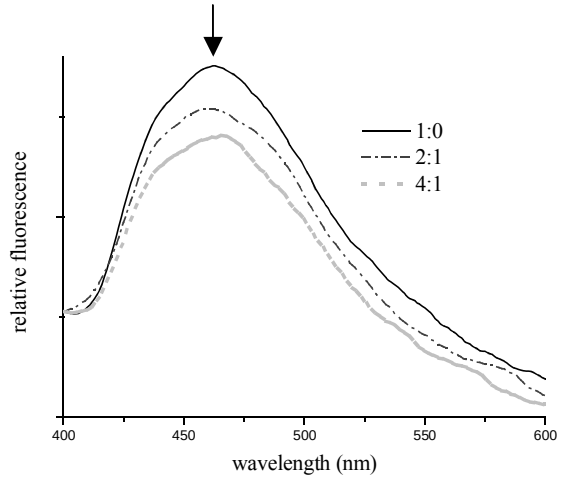

Fig. 3. Quenching of *cis*-[Pt(bapda)Cl_2] fluorescence emission upon titration with calf thymus DNA at various ratios (DNA base pairs:*cis*-[Pt(bapda)Cl_2])

As mentioned above, the cytotoxic activity of ligand bapda as compared to *cis*-[Pt(bapda)Cl_2] summarized in Table S2 (see Supporting Information) shows that the coordination of the carrier ligand to platinum improves slightly the biological activity. Ligand bapda was found to intercalate to the DNA, as well as its corresponding platinum(II) compound. Nevertheless, *cis*-[Pt(bapda)Cl_2] presents also the possibility of interacting with the N7 position of the guanine bases (Fig. 2), although this interaction appears to be strongly hindered.

3.7. Digital fluorescence microscopy

The cellular response of *cis*-[Pt(bapda)Cl_2] in A2780 and A2780R cells has been investigated and is compared to that of the ligand bapda. Incubation with both compounds,i.e. bapda and *cis*-[Pt(bapda)Cl_2] has been relatively short (15 min) due to the high cytotoxic activity in A2780 and A2780R cells; nevertheless, both compounds are able to enter into the cells after 15 min of incubation, and after 24 h the compounds are still visible inside the cells, with retention within large vesicles.

According to the cellular processing images of *cis*-[Pt(bapda)Cl_2] shown in Fig. 4, the distribution over time of the platinum(II) compound in A2780 and A2780R is slightly different.

Quickly after incubation with *cis*-[Pt(bapda)Cl_2] accumulation in A2780R cells in large vesicles is observed (Fig.4; D, E, and F). This accumulation remains constant over time up to 24 h after incubation (Fig. 5; A, B, C and D). In contrast, the cellular distribution of *cis*-[Pt(bapda)Cl_2] within the A2780 cell line changes over time (Fig. 4; A,B and C). After incubation with the compound, a fluorescence signal is visible in some vesicles close to the cell nucleus. However, three hours after the incubation *cis*-[Pt(bapda)Cl_2] is accumulated in vesicles extended over the cytosol. This accumulation remains visible 24 h after the incubation (Fig. 5; E, F, G and H). In both cell lines the large vesicles were identified as acidic lysosomes (Fig. 5) with the use of a specific stain (Lyso Tracker Red DND-99). In addition, as it is clear from the phase-contrast images, the number of vesicles around the nucleus present in the cell increases over time.

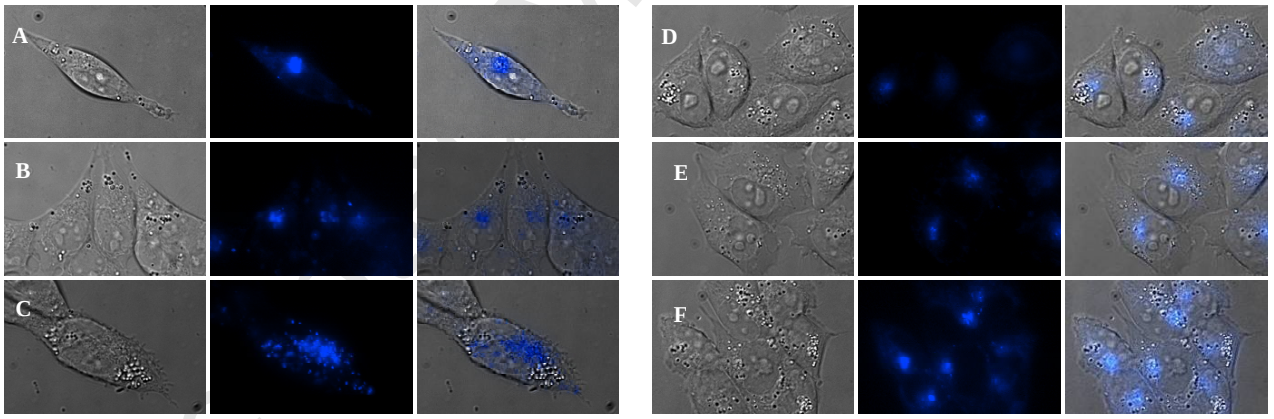

Fig. 4. Cellular distribution of *cis*-[Pt(bapda)Cl_2] in the A2780 cells (A, B and C) and in in the A2780R cells (D,E and F). Images A/D: 10 minutes after incubation time. Images B/E: 1 hour after incubation. Images C/F: 3 hours after incubation time. Phase-contrast images are shown on the left side, corresponding fluorescent images are in the middle, and superimposed images are on the right side.

Similar accumulation within acidic vesicles in A2780R cells of the ligand bapda and of *cis*-[Pt(bapda)Cl_2] was observed after incubation with bapda, and it remains visible 24 h after incubation (Fig. S4, Supporting Information). In contrast, the cellular distribution of ligand bapda in A2780 cells is slightly different, compared to that observed for *cis*-[Pt(bapda)Cl_2]. As shown in Fig. 6, the accumulation of bapda is less localized when imaging for a few minutes, 1 or 3 h after the incubation, while for its platinum(II) compound the accumulation is very specific (Fig. 4; A, B, and C)) after incubation. However, similar cellular processing 24 h after incubation with ligand bapda, compared to that of *cis*-[Pt(bapda)Cl_2] (Fig. 5) is observed in A2780 cells (Fig. S5, supporting Information). Both compounds are accumulated in acidic lysosomes, as shown from co-localization with Lyso Tracker Red DND-99, however, sequestration in additional vesicles in the A2780 cells is also observed.

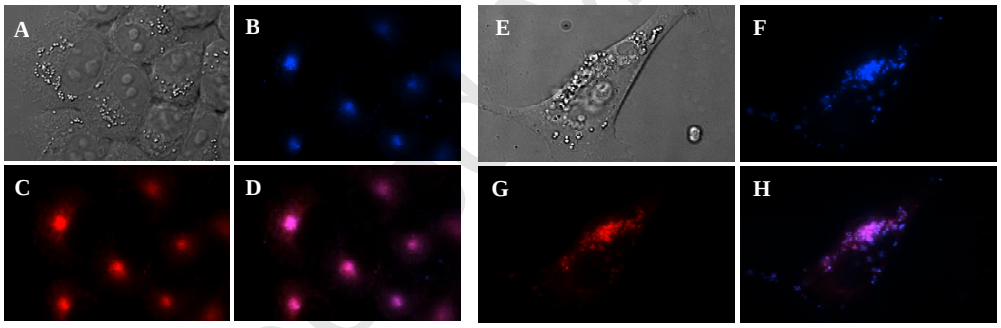

Fig. 5. Cellular distribution of *cis*-[Pt(bapda)Cl_2] in the A2780R cells (images A,B,C and D) and in the A2780 cells (images E, F, G and H) 24 h after incubation time, and staining with Lyso Tracker Red DND-99: (A/E) phase-contrast image of living A2780R/A2780 cells, respectively; (B/F) *cis*-[Pt(bapda)Cl_2] fluorescence (blue); (C/G) staining of lysosomes (red); (D/H) superimposed representation of the images of *cis*-[Pt(bapda)Cl_2] (blue) and Lyso Tracker Red DND-99 (red).

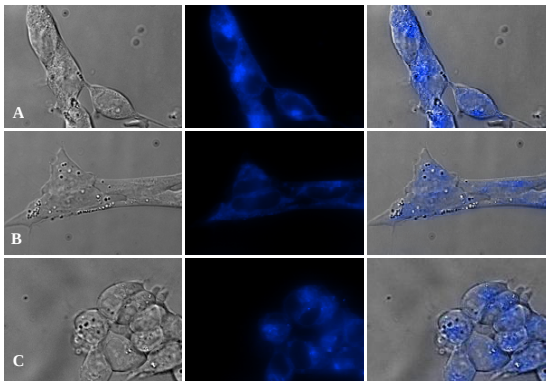

Fig. 6. Cellular distribution of ligand bapda in the A2780 cells. All the images were taken after the incubation period (15 minutes) had finished. Images A: 10 min after incubation time. Images B: 1 h after incubation. Images C: 3 h after incubation time. Phase-contrast images are shown on the left, corresponding fluorescent images are in the middle, and superimposed images are on the right.

To investigate whether glutathione facilitates the sequestration of these compounds into the lysosomes as a detoxification cell-mechanism, cellular processing of *cis*-[Pt(bapda)Cl_2] and bapda in GSH-depleted A2780R cells was followed over time. In correlation to the cytotoxic data, no changes in the cellular processing have been found related to *cis*-[Pt(bapda)Cl_2] treatment, where similar lysosomal accumulation could be observed in L-BSO treated or untreated A2780R cells (pictures not shown). However, differences in the cellular processing of bapda in L-BSO treated and untreated A2780R cells have been found (Fig. 7). This observation is also in agreement with the cytotoxic activity data (Table 2), where significant differences in the cytotoxic activity in A2780R and GSH-depleted A2780R cells were observed. The sequestration of the ligand bapda is visible over the cell in some vesicles different than acidic lysosomes (Fig. 7), as well as in the lysosomes.

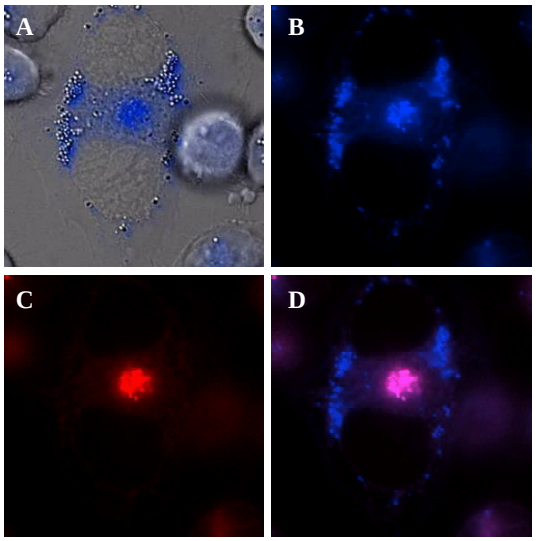

Fig. 7. A: Cellular distribution of bapda in depleted GSH A2780R cells 24 h after incubation time. Localization studies with Lyso Tracker Red DND-99: (A) phase-contrast image of living A2780 superimposed to bapda; (B) bapda fluorescence (blue); (C) staining of lysosomes (red); (D) superimposed representation of the images of bapda (blue) and Lyso Tracker Red DND-99 (red).

4. Discussion

A new fluorescent platinum(II) compound containing bapda as carrier ligand has been synthesized and characterized by several physical methods. The cytotoxic activities of both free ligand and *cis*-[Pt(bapda)Cl_2] show a high antiproliferative activity in A2780 and A2780R cells. The biological activity of *cis*-[Pt(bapda)Cl_2] is significantly different from that found for ligand bapda, suggesting that the coordination to platinum(II) ion improves the activity of bapda. However, cross-resistance to platinum has been found for *cis*-[Pt(bapda)Cl_2] against A2780R cells. As it is well known, the inactivation of platinum(II) compounds by GSH or MT molecules is an important resistance mechanism [26]. However, the GSH inactivation does not seem to play an important role towards cross-resistance to platinum found for *cis*-[Pt(bapda)Cl_2] during the *in vitro* studies presented herein, since no significant changes have been observed between GSH-depleted A2780R cells and normal A2780R cells. In addition, the reaction between GSH and *cis*-

[Pt(bapda)Cl_2] (1:4) was investigated by ^{195}Pt NMR spectroscopy for the first 24 h, and no reaction was observed. This observation confirm that GSH cannot react with *cis*-[Pt(bapda)Cl_2]. Moreover, cationic 1,1/t,t type platinum(II) compounds that reacted with GSH by the displacement of the chlorides and subsequent degradation of the compound by the replacement of the diaminealkyl linker [18]. However, in the case of *cis*-[Pt(bapda)Cl_2], the carrier ligand is coordinated in a chelating fashion way. Thus, the stability of this new platinum(II) compound is expected to be higher against GSH inactivation.

Cellular processing studies of *cis*-[Pt(bapda)Cl_2] in A2780R cells with fluorescence microscopy show accumulation in acidic lysosomes after short incubation, which could be attributed to the resistant mechanisms. Several examples of such accumulation of platinum(II) compounds are reported in the literature [6-10]. Interestingly, dinuclear platinum(II) compounds containing anthraquinone ligands trapped in lysosomal vesicles were previously reported [6], and accumulation in A2780R cells was found constant over time, which was not observed for the sensitive cell line A2780. This observation suggested that the vesicular sequestration was due to a resistance mechanism present in the A2780R cells. However, in the same studies, after 24 h of incubation with the corresponding ligand no vesicles containing the compounds were observed [6], suggesting that the sequestration in acidic vesicles in A2780R cell line is a specific response to the corresponding platinum compound [6]. In the case of cellular processing of *cis*-[Pt(bapda)Cl_2] and bapda in A2780R cells, fast sequestration after short incubation in acidic lysosomes is observed, which suggests that it is not a specific cellular response to the platinum compound. Moreover, accumulation of *cis*-[Pt(bapda)Cl_2] in acidic lysosomes in A2780 cells has been observed as well, indicating that this sequestration might not be related to resistance mechanisms. Putting all together, these observations suggest that the lysosomal sequestration is a detoxification mechanisms of the cells to *cis*-[Pt(bapda)Cl_2] and bapda. Organic drugs, such as daunorubicin and mitoxantrone were found to be accumulated in acidic vesicles [27], which indicates that this might be a protective

response of the cells to different external agents. Moreover, the cellular distribution of *cis*-[Pt(bapda)Cl_2] and bapda in A2780 cells appears to be slightly different. Three hours after incubation with *cis*-[Pt(bapda)Cl_2] lysosomal sequestration of this platinum(II) compound was observed. The free ligand is sequestered within lysosomes as well; however, this was not observed within the first 3 h after the incubation, suggesting that the detoxification mechanisms of A2780 cells respond differently to the platinum(II) compound.

As it has been reported previously, the glutathione is involved in the excretion and/or sequestration of toxic compounds as a cellular protection system [28]. To investigate whether glutathione facilitates sequestration of *cis*-[Pt(bapda)Cl_2] in lysosomes, the fluorescent microscopy in GSH-depleted A2780R cells has been investigated and compared to that in normal A2780R cells. The cellular processing of *cis*-[Pt(bapda)Cl_2] in GSH-depleted A2780R cells shown no significant differences as compared to the same studies in normal A2780R cells. This observation correlates with the cytotoxic activity data of *cis*-[Pt(bapda)Cl_2] in normal A2780R cells and in GSH -depleted A2780R cells, where no significant differences were found between the EC_{50} values. Therefore, the sequestration of *cis*-[Pt(bapda)Cl_2] after short-time incubation in lysosomes seems to be not related to the GSH levels, and might indicate a specific drug uptake pathway, such as endocytosis. To elucidate this behavior in detail, further studies are in progress and will be published elsewhere. In contrast, a quite different cellular processing has been observed with the ligand bapda in GSH-depleted A2780R cells, where an increased number of different vesicles are visible in the cells after incubation with bapda (Fig. 6). This suggests that the cellular processing of the ligand bapda is influenced by the concentration of GSH in A2780R cells. This is also correlated with the cytotoxic activity data, where significant differences between cytotoxic activity of bapda in normal A2780R cells and GSH-depleted A2780R cells.

In addition to the *in vitro* studies and because it is believed that the main target of platinum compounds is the DNA, two different approaches to elucidate the reactivity of *cis*-[Pt(bapda)Cl_2]

with the DNA have been performed. The interaction of *cis*-[Pt(bapda)Cl_2] with the 9-EtG was investigated by ^{1}H and ^{195}Pt-NMR spectroscopy. After 12 days reaction it can be concluded that the steric protection around the platinum(II) ion most likely hampers the 9-EtG approaches to the metal ion. Nevertheless, it is clear that small amounts of [Pt(bapda)(9-EtG)Cl] species are formed. Moreover, related platinum compounds with ethyl substituents on the amine groups have been described in the literature [29], and were found to be cytotoxic against several cell lines in the absence of the intercalating groups, compared to *cis*-[Pt(bapda)Cl_2]. These results, together with the low reactivity of *cis*-[Pt(bapda)Cl_2] towards 9-EtG and low cross-resistance with cisplatin, suggest that the biological activity of this new platinum(II) compound stems primarily from the anthracene groups. In the literature interesting classes of organic molecules, so-called bisintercalators [30], have been synthesized by linking two heterocycles with chains of varying lengths between the intercalator moieties [31]. Such special molecules have been investigated successfully as carrier ligands in the synthesis of new platinum(II) antitumor agents [32]. Thus, the *cis*-[Pt(bapda)Cl_2] may intercalate with the anthracene ring between the DNA base pairs. Moreover, it has been previously reported fluorescence quenching experiment, where small amounts of a concentrated stock solution of pBR322 plasmid DNA [6] or calf thymus DNA [10] were added to the solutions of fluorescent platinum(II) compounds to investigate the possible intercalative properties of such molecules. Similar studies has been performed with *cis*-[Pt(bapda)Cl_2], with a significant decrease in the emission spectrum after the addition of calf thymus DNA. This observation suggests that the anthracene rings of *cis*-[Pt(bapda)Cl_2] intercalate between the DNA base pairs.

The data reported herein is a useful baseline for future studies with *cis*-[Pt(bapda)Cl_2]. The cellular accumulation and DNA platination of *cis*-[Pt(bapda)Cl_2] are of high interest, since decreased uptake and increased tolerance to DNA damage have been found to be involved in the resistance mechanisms of several platinum-based drugs. These studies are in progress and will be reported elsewhere.

Acknowledgments

This work has been performed under the auspices of the Graduate Research School HRSMC, a joint activity of Leiden University and the two Universities in Amsterdam. This research has been financially supported by the Council for Chemical Sciences of The Netherlands Organization for Scientific Research (CW-NWO). The support and sponsorship concerted by COST Actions D39/0006/02 and D39/0005/11 is kindly acknowledged. The authors thank Johnson & Matthey (Reading, UK) for their generous loan of K_2PtCl_4. The cytotoxicity test of the compounds was generously supported by PCN (Tavapharmachemie) The Netherlands. Fons Lefeber, Jos van Brussel, John A.P.P. van Dijk and Jopie A. Erkelens-Duijndam are acknowledged for assistance with the NMR techniques, for the C, H and N analyses, and for the ESI-MS determinations, respectively. The authors would like to acknowledge Simon Contaldi for useful discussions. Both A2780 cell lines were kindly provided by Prof. Dr. Carmen Navarro-Ranninger (Universidad Autonoma de Madrid, Spain).

Supporting Information Available: Table S1. Crystal data and structure refinement details for *cis*-Pt(bapda)Cl_2, Table S2. IC_{50} values in ! M of compound *cis*-[Pt(bapda)Cl_2)] and bapda comparing to cisplatin on human tumor cell lines after 5 days incubation, Fig. S1. PLATON/POVRAY view of *cis*-[Pt(bapda)Cl_2] π-π stacking interaction between two anthracyl rings and the hydrogen bonding, Fig. S2. ^{195}Pt NMR spectrum (300 MHz) of *cis*-[Pt(bapda)Cl_2)] in DMF-d_7 at 310 K reacted with 2 eq. 9-EtG 24 h after mixed, Fig. 3. ESI-MS spectrum of *cis*-[Pt(bapda)Cl_2)] in DMF-d_7 at 310 K reacted with 9-EtG 24 h after mixed, Fig. S4. Cellular distribution of bapda in the A2780R cells 24 h after incubation time, and Fig. S5. Cellular distribution of bapda in the A2780 cells 24 h after incubation time. This material is available free of charge via the Internet at http://pubs.acs.org.

The CIF file for compound *cis*-[Pt(bapda)Cl_2] (CCDC 711124) giving full X-ray crystallographic data can be obtained free of charge from The Cambridge Crystallographic Data Centre via www.ccdc.cam.ac.uk/data_request/cif.

References

[1] Boulikas T, Vougiouka M. Cisplatin and platinum drugs at the molecular level (review). Oncol. Rep 2003;10:1663-82.

[2] Reedijk J. Metal-Ligand Exchange kinetics in Platinum and Ruthenium Complexes. Platinum Metals Rev 2008;52:2-11.

[3] Molenaar C, Teuben JM, Heetebrij RJ, Tanke HJ, Reedijk J. New insights in the cellular processing of platinum antitumor compounds, using fluorophore-labeled platinum complexes and digital fluorescence microscopy. J Biol Inorg Chem 2000;5:655-65.

[4] Kalayda GV, Wagner CH, Buss I, Reedijk J, Jaehde U. Altered localisation of the copper efflux transporters ATP7A and ATP7B associated with cisplatin resistance in human ovarian carcinoma cells. BMC Cancer 2008;8:1471-2407.

[5] Safaei R, Katano K, Larson BJ, Samimi G, Holzer AK, Naerdemann W, et al. Intracellular localization and trafficking of fluorescein-labeled cisplatin in human ovarian carcinoma cells. Clin Cancer Res 2005;11:756-67.

[6] Jansen BAJ, Wielaard P, Kalayda GV, Ferrari M, Molenaar C, Tanke HJ, et al. Dinuclear platinum complexes with N,N '-bis(aminoalkyl)-1,4-diaminoanthraquinones as linking ligands. Part I. Synthesis, cytotoxicity, and cellular studies in A2780 human ovarian carcinoma cells. J Biol Inorg Chem 2004;9:403-13.

[7] Kalayda GV, Jansen BAJ, Molenaar C, Wielaard P, Tanke HJ, Reedijk J. Dinuclear platinum complexes with N,N '-bis(aminoalkyl)-1,4-diaminoanthraquinones as linking ligands. Part II. Cellular processing in A2780 cisplatin-resistant human ovarian carcinoma cells: new insights into the mechanism of resistance. J Biol Inorg Chem 2004;9:414-22.

[8] Kalayda GV, Jansen BAJ, Wielaard P, Tanke HJ, Reedijk J. Dinuclear platinum anticancer complexes with fluorescent N,N'-bis(aminoalkyl)-1,4-diaminoanthraquinones: cellular processing in two cisplatin-resistant cell lines reflects the differences in their resistance profiles. J Biol Inorg Chem 2005;10:305-15.

[9] Kalayda GV, Zhang GF, Abraham T, Tanke HJ, Reedijk J. Application of fluorescence microscopy for investigation of cellular distribution of dinuclear platinum anticancer drugs. J Med Chem 2005;48:5191-202.

[10] Alderden RA, Mellor HR, Modok S, Hambley TW, Callaghan R. Cytotoxic efficacy of an anthraquinone linked platinum anticancer drug. Biochem Pharmacol 2006;71:1136-45.

[11] Akdi K, Vilaplana RA, Kamah S, Gonzalez-Vilchez F. Effects of Tris and Hepes buffers on the interaction of palladium-diaminopropane complexes with DNA. J Inorg Biochem 2005;99:1360-8.

[12] Appleton TG, Hall JR. Complexes With 6 Membered Chelate Rings.VI. Proton Magnetic-Resonance Study Of Some Platinum(II) Complexes Of N,N'-Dimethylpropane-1,3-Diamine,N,N,N','N'-Tetramethylpropane-1,3-Diamine, And N,N,N',N'-Tetramethylethylenediamine. Inorg Chem 1972;11:124.

[13] Appleton TG, Hall JR. Complexes With 6-Membered Chelate Rings.I. Preparation Of Platinum(II) And Palladium(II) Complexes Of Trimethylenediamine And Some Methyl-Substituted Derivatives. Inorg Chem 1970;9:1800-6.

[14] Zhang GQ, Yang GQ, Wang SQ, Chen QQ, Ma JS. A highly fluorescent anthracene-containing hybrid material exhibiting tunable blue-green emission based on the formation of an unusual "T-shaped" excimer. Chem-Eur J 2007;13:3630-5.

[15] BRUCK AXS INC C. 2002.

[16] SHELX-TL, Bruker AXS. Madison, Wisconsin, USA, 2004.

[17] Patricia Marqués-Gallego, Ganna V. Kalayda, Ulrich Jaehde, Hans den Dulk, Jaap Brouwer, Reedijk J. Cellular accumulation and DNA platination of two new platinum(II) anticancer compounds based on anthracene derivatives as carrier ligands. J Inorg Biochem 2009, in press.

[18] Jansen BAJ, Brouwer J, Reedijk J. Glutathione induces cellular resistance against cationic dinuclear platinum anticancer drugs. J Inorg Biochem 2002;89:197-202.

[19] Keepers YP, Pizao PE, Peters GJ, Vanarkotte J, Winograd B, Pinedo HM. Comparison Of The Sulforhodamine-B Protein And Tetrazolium (MTT) Assays For In vitro Chemosensitivity Testing. Eur J Cancer 1991;27:897-900.

[20] Patricia Marqués-Gallego, Hans den Dulk, Jaap Brouwer, Huub Kooijman, Anthony L. Spek, Olivier Roubeau, et al. Synthesis, crystal structure, studies in solution and cytotoxicity of two new fluorescent platinum(II) compounds containing anthracene derivatives as a carrier ligand. Inorg Chem 2008;47:11171-9.

[21] Pregosin PS. Pt-195 Nuclear Magnetic-Resonance. Coord Chem Rev 1982;44:247-91.

[22] Odoko M, Okabe N. Dichloro(propane-1,3-diamine-!^{2} N,N')platinum(II), dichloro(propane-1,3-diamine-!^{2} N,N')palladium(II) and ! -4,9-diazadodecane-1,12-diamine-!^{2} N',N^{4}:-!^{2} N^{9},N^{12}-bis[dichloroplatinum(II)]. Acta Crystallogr Sec C-Cryst Struct Commun 2006;62:M136-M9.

[23] Lempers ELM, Inagaki K, Reedijk J. Reactions Of [PtCl(Dien)]Cl With Glutathione, Oxidized Glutathione And S-Methyl Glutathione - Formation Of An S-Bridged Dinuclear Unit. Inorganica Chimica Acta-Bioinorganic Chemistry 1988;152:201-7.

[24] Reedijk J. Why does cisplatin reach guanine-N7 with competing S-donor ligands available in the cell? Chem Rev 1999;99:2499-510.

[25] Vanboom SSGE, Reedijk J. Unprecedented Migration Of $[Pt(dien)]^{2+}$ (Dien = 1,5-Diamino-3-Azapentane) From Sulfur To Guanosine-N7 In S-Guanosyl-L-Homocysteine (sgh). J Chem Soc-Chem Commun 1993:1397-8.

[26] Rabik CA, Dolan ME. Molecular mechanisms of resistance and toxicity associated with platinating agents. Cancer Treat Rev 2007;33:9-23.

[27] Merlin JL, Bour-Dill C, Marchal S, Ramacci C, Poullain MG, Giroux B. Modulation of daunorubicin cellular resistance by combination of P-glycoprotein blockers acting on drug efflux and intracellular drug sequestration in golgi vesicles. Cytometry 2000;41:62-72.

[28] Ishikawa T, Li ZS, Lu YP, Rea PA. The GS-X pump in plant, yeast, and animal cells: Structure, function, and gene expression. Biosci Rep 1997;17:189-207.

[29] Vickery K, Bonin AM, Fenton RR, Omara S, Russell PJ, Webster LK, et al. Preparation, Characterization, Cytotoxicity, And Mutagenicity Of A Pair Of Enantiomeric Platinum(II) Complexes With The Potential To Bind Enantioselectively To DNA. J Med Chem 1993;36:3663-8.

[30] Dawson S, Malkinson JP, Paumier D, Searcey M. Bisintercalator natural products with potential therapeutic applications: isolation, structure determination, synthetic and biological studies. Nat Prod Rep 2007;24:109-26.

[31] Becker MM, Dervan PB. Molecular Recognition Of Nucleic-Acid By Small Molecules - Binding-Affinity And Structural Specificity Of Bis-(Methidium)Spermine. J Am Chem Soc 1979;101:3664-6.

[32] Perez JM, Lopez-Solera I, Montero EI, Brana MF, Alonso C, Robinson SP, et al. Combined effect of platination and intercalation upon DNA binding of novel cytotoxic Pt-bis(naphthalimide) complexes. J Med Chem 1999;42:5482-6.